

Received July 24, 2020, accepted August 5, 2020, date of publication August 19, 2020, date of current version August 31, 2020.

Digital Object Identifier 10.1109/ACCESS.2020.3017708

A Novel ITI Suppression Technique for Coded Dual-Track Dual-Head Bit-Patterned Magnetic Recording Systems

SANTI KOONKARNKHAI¹, CHANON WARISARN², (Member, IEEE),
AND PIYA KOVINTAVEWAT¹, (Member, IEEE)

¹Advanced Signal Processing for Disruptive Innovation Research Center, Nakhon Pathom Rajabhat University, Nakhon Pathom 73000, Thailand

²College of Advanced Manufacturing Innovation, King Mongkut's Institute of Technology Ladkrabang, Bangkok 10520, Thailand

Corresponding authors: Chanon Warisarn (chanon.wa@kmitl.ac.th) and Piya Kovintavewat (piya@npru.ac.th)

This work was supported in part by the Research and Development Institute, Nakhon Pathom Rajabhat University, Thailand, under Grant GP_62_12, and in part by the College of Advanced Manufacturing Innovation, King Mongkut's Institute of Technology Ladkrabang, Thailand, under Grant KREF146206.

ABSTRACT Generally, an intertrack interference (ITI) is a critical problem in bit-patterned magnetic recording (BPMR) systems that can attain an areal density (AD) up to 4 Tb/in². Unavoidably, at high ADs, a very narrow track width must be employed, leading to severe ITI and unacceptable system performance. To tackle the ITI; therefore, this article introduces a novel ITI suppression technique for coded dual-track dual-head (DTDH) BPMR systems. At the first turbo iteration, the weighted readback signal of the adjacent track served as an estimated ITI signal is utilized for subtracting from the target readback signal to subside the ITI effect, before passing the refined readback signal to a turbo equalizer. Nonetheless, for the second turbo iteration onwards, the estimated ITI signal generated by the soft information obtained from a decoder at each turbo iteration will be then employed to subtract from the target readback signal during the turbo decoding process. Computer simulation results demonstrate that the proposed system can provide better performance than the DTDH system using a hard ITI suppression technique as well as the conventional system using one read head to decode one data track for all ADs, because the proposed technique can estimate the ITI signal well. Furthermore, when considering the recording system under the effects of media noise and track mis-registration, we also found that the proposed system is more robust than other systems.

INDEX TERMS Bit-patterned magnetic recording, ITI suppression, soft information, turbo decoding.

I. INTRODUCTION

A current perpendicular magnetic recording (PMR) technology used to store data in hard disk drives is approaching its limit at 1 Terabit per square inch (Tb/in²), technically known as a super-paramagnetic limit [1]. To continuously support the need for storing enormous data in a digital era, one of the promising recording technologies called a bit-patterned magnetic recording (BPMR) has been introduced, which can achieve an areal density (AD) up to 4 Tb/in². Additionally, when the BPMR technology is combined with a heat-assisted magnetic recording technology, we obtain a heated-dot magnetic recording (HDMR) technology that can expand the AD up to 10 Tb/in² [2]. Unlike PMR, BPMR stores one data bit on each magnetic island separated by non-magnetic material [1],

The associate editor coordinating the review of this manuscript and approving it for publication was Wei Wang¹.

which helps reduce the transition noise as existed in a granular medium. Therefore, this article focuses on a BPMR medium with a rectangular array arrangement as shown in Fig. 1.

Generally, a read head is employed to sense an induced magnetization from the magnetic island. Because the size of read head is normally larger than the island, it covers many islands while reading data in both along- and cross-track directions. This definitely causes the readback signal to experience with both intersymbol interference (ISI) and inter-track interference (ITI) [3], whose severity depends on an operating AD. Specifically, the larger the AD, the more severe the ISI and ITI. In addition, other disturbances can also degrade the BPMR system performance, such as track mis-registration (TMR), media noise, write synchronization error [4], and skew angle [5]. The TMR is a head offset in either upward or downward direction that is occurred when the center of the read head is not aligned with that of the

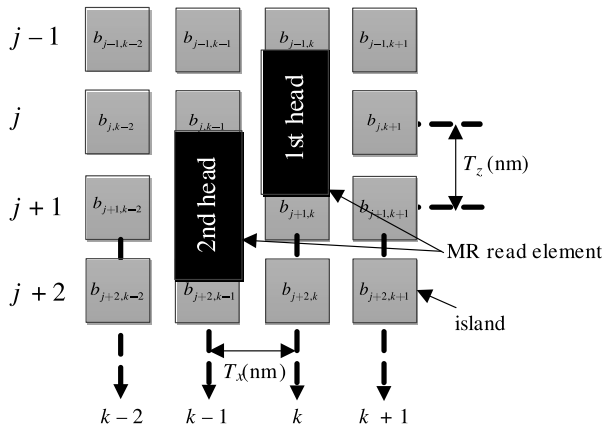


FIGURE 1. A medium with regular island arrangement for the DTDH detection technique.

target track, whereas the nature of media noise is caused by the fluctuation of the island size, location, and magnetic saturation. Moreover, the write synchronization error results from mis-synchronization between the write clock and the bit island, leading to a crucial problem of insertion, deletion and substitution errors [4], [6], which can cause many errors in a data detection process. Finally, the skew angle is occurred when the angle of the read head is not aligned with the target track direction, this deteriorates the system performance if precaution is not taken to prevent it [7].

Several researchers have proposed the methods to mitigate the ITI effect in a BPMR system. For example, Nabavi and Kumar [3] developed the two-dimensional (2D) pulse response to represent the BPMR channel and proposed a 2D equalizer to combat ISI and ITI, where the system employed three read heads to scan three data tracks and decoded only the main data track. Next, Nabavi *et al.* [8] proposed a modified Viterbi detector, whose trellis has 4 states with 3 parallel branches between any two connected states, to alleviate the ITI embedded in the readback signal. The design of iterative decision feedback detection and 2D generalized partial response (GPR) equalization based on minimum mean-squared error (MMSE) followed by one-dimensional (1D) Viterbi algorithm [9] was also introduced and evaluated its performance under several ADs. This technique was claimed that it is a good candidate for an ultra-high capacity BPMR system. Then, Karakulak [10] presented the full-complexity 2D Viterbi detector, whose trellis has 64 states with 8 incoming/outgoing branches, to tackle the ITI, which can perform better than other 2D Viterbi detectors at an expense of high complexity.

Furthermore, Warisarn *et al.* [11] and Kovintavewat *et al.* [12] utilized a 2D modulation code to avoid fatal data patterns that cause severe ITI to be stored on a magnetic medium; however, these methods required large memory to encode and decode the data. Hence, Chang and Cruz [13] employed the joint track concept to design the equalizer suitable for a staggered BPMR system, whereas Fujii and Shinohara [14] proposed the ISI and ITI cancellation technique by using

a multi-track iterative method for a shingled write recording system. Yao *et al.* [15] proposed and analyzed the 2D maximum-likelihood page detection to cope with the ISI and ITI effects in BPMR and page-oriented optical memory systems. Moreover, an array-reader-based magnetic recording approach [16] was presented to enhance recording capacity for both BPMR and 2D magnetic recording technologies, where multiple readback signals were utilized to process altogether. For example, the design of 2D equalizer was proposed by jointly processing based on an array-reader two-track detection system [17], whose performance gain can be achieved over a traditional single-reader single-track detection system. Finally, Koonkarnkhai and Kovintavewat [18] introduced a simple ITI mitigation for a 2-head 2-track (2H2T) BPMR channel, where two read heads were employed to read two data tracks and decoded them simultaneously. To subside the ITI, we subtracted the weighted readback signal of the 2nd track (acted as an ITI signal) from the 1st readback signal, and vice versa.

Nowadays, a modern signal processing technique for magnetic recording systems usually utilizes a multi-track multi-head concept that performs together with the turbo decoding process [19] to boost the system performance [14], [20], [21]. For instance, Koonkarnkhai *et al.* [20] introduced an iterative 2H2T detection method for a staggered BPMR system to lessen the ITI effect. To do so, at the first iteration, we subtracted the weighted readback signal obtained from the adjacent tracks (served as an estimated ITI signal) from the target readback signal, before passing the refined readback signal to the turbo decoder. Thus, at the second iteration onwards, the estimated ITI signal was reconstructed by the hard decision received from the output of the turbo decoder.

Nonetheless, this article presents a novel ITI suppression technique for a coded DTDH BPMR channel with regular island arrangement, which is an extended work from [22], where we thoroughly explain the proposed ITI suppression technique on how it operates and investigate its performance more in the presence of media noise and TMR. Specifically, the proposed technique employs two read heads to read two data tracks and decode them concurrently at the receiver side. Hence, the log-likelihood ratios (LLRs) of the coded bits obtained from the low-density parity-check (LDPC) decoder [23] are utilized to produce the weighted readback signals before subtracting them from the target readback signals. The proposed system can provide better bit-error rate (BER) performance if compared to the DTDH system with hard ITI suppression technique [20] and the conventional system for all ADs, particularly when the recording system severely encounters both media noise and TMR.

The rest of this article is organized as follows. The BPMR channel model for the proposed scheme is explained in Section II. Section III describes how the proposed system performs and summarizes the design of a 2×3 target and its compatible 1D equalizer. The performance of the proposed system will be investigated in Section IV. Finally, Section V gives the conclusion.

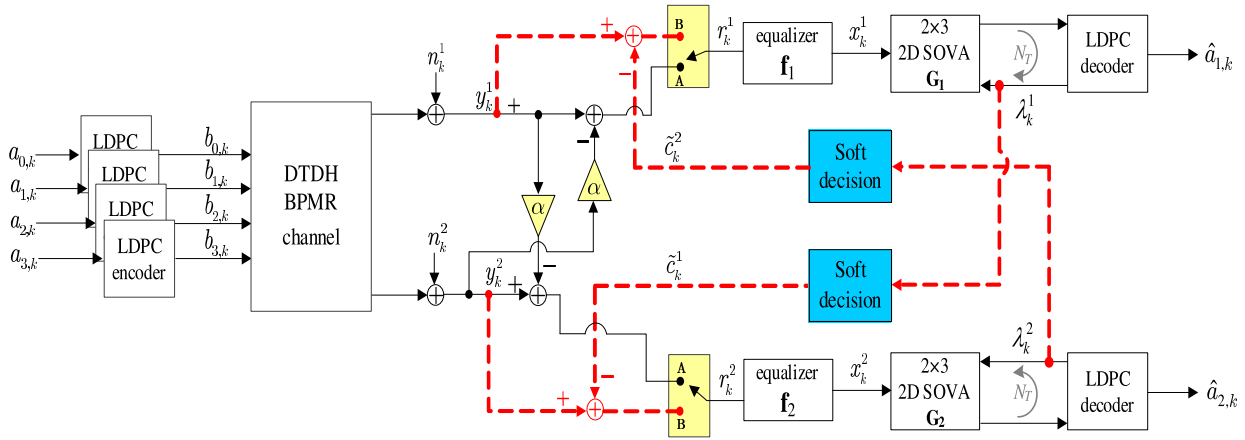


FIGURE 2. A DTDH BPMR channel model with the soft ITI suppression technique.

II. CHANNEL MODEL

Consider the coded BPMR system with the proposed ITI suppression technique in Fig. 2. A binary input data sequence $\{a_{j,k}\}$ is encoded by a rate-8/9 LDPC encoder [23] to obtain a sequence $\{b_{j,k}\}$, where $j = m$ is the target track, $m \in \{1, 2\}$ is the m th read head, and $j = m - 1, m + 1$ is the adjacent track. Subsequently, a coded sequence $\{b_{j,k}\}$ is fed to the BPMR channel. For simplicity, we assume that the m th read head will read data on the m th track. Generally, the readback signal of the m th read head corrupted by ITI and ISI can be written as

$$y_k^m = \sum_{j=-\infty}^{\infty} \sum_{i=-\infty}^{\infty} h_{j,i} b_{m-j,k-i} + n_k^m, \quad (1)$$

where $h_{j,i}$'s are the coefficients of the 2D channel response, which can be acquired by sampling the 2D Gaussian pulse response [3] at integer multiples of a bit pitch (T_x) and a track pitch (T_z), and n_k^m is additive white Gaussian noise with zero mean and variance σ^2 associated with the m th read head.

Practically, the 2D Gaussian pulse response corrupted by media noise and TMR can be modeled as

$$H(z + \Delta_T, x) = A \exp \left(-\frac{1}{2} \left[\left(\frac{x + \Delta_x}{cW_x} \right)^2 + \left(\frac{z + \Delta_T + \Delta_z}{cW_z} \right)^2 \right] \right), \quad (2)$$

where $A = 1$ is a normalized peak amplitude of the 2D pulse response, W_z and W_x are the pulse-width-at-half-maximum (PW₅₀) of the cross- and along-track pulses, respectively, $c = 1/2.3458$ is a constant to account for the relationship between PW₅₀ and the standard deviation of a Gaussian function, Δ_x is the along-track location fluctuation, Δ_z is the cross-track location fluctuation. Note that this article only considers the media noise resulted from the location fluctuation, which will be referred to as ‘‘position jitter noise.’’ Hence, we model the media noise or position jitter noise (Δ_x and Δ_z) as a truncated Gaussian probability distribution function with zero mean and variance σ_j^2 , where σ_j is

specified as the percentage of T_x . Additionally, Δ_T is the head-offset or the distance between the center of the target track and that of the read head, where the percentage of TMR is defined as

$$\text{TMR} (\%) = \frac{\Delta_T}{T_z} \times 100. \quad (3)$$

At the receiver, the readback signals $\{y_k^m\}$ are fed to the equalizers followed by the turbo decoding process, which iteratively exchanges the soft information between the 2D soft-output Viterbi algorithm (SOVA) [24] and the LDPC decoder for N_T iterations. In this article, the LDPC decoder is implemented based on a message-passing algorithm with N_i internal iteration [23], where $N_i = 3$ is considered.

III. PROPOSED SCHEME

This section explains how the proposed ITI suppression technique operates and briefly summarizes how to design the 2D target and its compatible 1D equalizer. In [20], the ITI suppression technique for the coded DTDH BPMR channel with a staggered array island medium was presented, which employed the hard decision from the LDPC decoder to estimate the ITI signal. To improve its performance further, this article proposes to utilize the soft information from the LDPC decoder to approximate the ITI signal for the BPMR channel with a regular array island medium [22].

Before explaining the proposed technique, we first assume that the read head reads the k th bit on the j th track, where the ISI is restricted to two adjacent symbols ($k - 1$) and ($k + 1$), and the ITI is limited to two adjacent tracks ($j - 1$) and ($j + 1$). Thus, we can consider $\{i, j\} \in \{\pm 1, 0\}$ in (1). Then, the 2D channel pulse response can be illustrated in a matrix form as

$$H(jT_z, iT_x) = \mathbf{H} = \begin{bmatrix} \mathbf{h}_{-1} \\ \mathbf{h}_0 \\ \mathbf{h}_1 \end{bmatrix} = \begin{bmatrix} h_{-1,-1} & h_{-1,0} & h_{-1,1} \\ h_{0,-1} & h_{0,0} & h_{0,1} \\ h_{1,-1} & h_{1,0} & h_{1,1} \end{bmatrix}, \quad (4)$$

where $h_{0,0} = 1$ is supposed to be a normalized peak amplitude, $h_{-1,0}$ and $h_{1,0}$ represent the ITI, and $h_{0,-1}$ and $h_{0,1}$ represent the ISI.

A. SOFT ITI SUPPRESSION TECHNIQUE

Suppose the proposed technique utilizes two read heads to read the data from track $j = 1$ and $j = 2$ that corresponds to the input data sequences $\{a_{1,k}\}$ and $\{a_{2,k}\}$, respectively, where $\{a_{0,k}\}$ and $\{a_{3,k}\}$ are considered as random data sequences. For simplicity, we assume a symmetric BPMR channel and the read heads are placed at the center of their tracks. Thus, we can employ $h_{1,1} = h_{-1,-1} = h_{-1,1} = h_{1,-1}$, $h_{1,0} = h_{-1,0}$, and $h_{0,1} = h_{0,-1}$ [8]. Note that if the read heads are positioned more towards inner tracks j and $j+1$, we found that the system performance will be degraded (not shown here). This might be because although the ITI from tracks $j - 1$ and $j + 2$ is reduced, the amplitude of the target signal is decreased and the ITI from tracks j and $j+1$ is also increased, thus lowering the quality of the readback signals. Therefore, the performance is deteriorated as the read head is moved away from its original position at the center of the track, which is similar to the result in [16].

At the first turbo iteration ($N_T = 1$), the switches in Fig. 2 are at the position **A**. To mitigate the ITI embedded in the 1st readback signal, we subtract the weighted version of the 2nd readback signal from the 1st readback signal. Similarly, to subside the ITI embedded in the 2nd readback signal, we subtract the weighted version of the 1st readback signal from the 2nd readback signal. This process is similar to [18], [20], where the refined readback signal in the noiseless channel of the 1st read head scanning the j th track can be written as

$$\begin{aligned} r_k^1 &= y_k^1 - \alpha y_k^2, \\ &= h_{1,1}b_{j-1,k+1} + h_{1,0}b_{j-1,k} + h_{1,1}b_{j-1,k-1} + h_{0,1}b_{j,k+1} \\ &\quad + b_{j,k} + h_{0,1}b_{j,k-1} - \alpha h_{1,1}b_{j,k+1} - \alpha h_{1,0}b_{j,k} \\ &\quad - \alpha h_{1,1}b_{j,k-1} - \alpha h_{1,1}b_{j+2,k+1} - \alpha h_{1,0}b_{j+2,k} \\ &\quad - \alpha h_{1,1}b_{j+2,k-1} + (h_{1,1} - \alpha h_{0,1})b_{j+1,k+1} \\ &\quad + (h_{1,0} - \alpha)b_{j+1,k} + (h_{1,1} - \alpha h_{0,1})b_{j+1,k-1}, \end{aligned} \quad (5)$$

and that of the 2nd read head scanning the $(j + 1)$ th track can be expressed as

$$\begin{aligned} r_k^2 &= y_k^2 - \alpha y_k^1, \\ &= h_{0,1}b_{j+1,k+1} + b_{j+1,k} + h_{0,1}b_{j+1,k-1} + h_{1,1}b_{j+2,k+1} \\ &\quad + h_{1,0}b_{j+2,k} + h_{1,1}b_{j+2,k-1} - \alpha h_{1,1}b_{j-1,k+1} \\ &\quad - \alpha h_{1,0}b_{j-1,k} - \alpha h_{1,1}b_{j-1,k-1} - \alpha h_{1,1}b_{j+1,k+1} \\ &\quad - \alpha h_{1,0}b_{j+1,k} - \alpha h_{1,1}b_{j+1,k-1} + (h_{1,1} - \alpha h_{0,1})b_{j-1,k+1} \\ &\quad + (h_{1,0} - \alpha)b_{j,k} + (h_{1,1} - \alpha h_{0,1})b_{j,k-1}, \end{aligned} \quad (6)$$

where α is a weighting factor. It has been shown in [18] that a good weighting factor can be easily obtained from

$$\alpha = \frac{h_{1,0}}{h_{0,0}} = \frac{h_{1,1}}{h_{0,1}} = \exp\left(-0.5\left(\frac{T_z}{cW_z}\right)^2\right). \quad (7)$$

Because $\alpha h_{1,0} \approx 0$ and $\alpha h_{1,1} \approx 0$, which can be neglected, the refined readback signals after the ITI suppression technique of the 1st and 2nd read heads (i.e., (5) and (6)) can be reduced to

$$\begin{aligned} r_k^1 &= \underbrace{h_{1,1}b_{j-1,k+1} + h_{1,0}b_{j-1,k} + h_{1,1}b_{j-1,k-1}}_{\text{ITI signal from the } (j-1)\text{th track}} \\ &\quad + \underbrace{h_{0,1}b_{j,k+1} + b_{j,k} + h_{0,1}b_{j,k-1}}_{\text{wanted signal}}, \end{aligned} \quad (8)$$

and

$$\begin{aligned} r_k^2 &= \underbrace{h_{0,1}b_{j+1,k+1} + b_{j+1,k} + h_{0,1}b_{j+1,k-1}}_{\text{wanted signal}} \\ &\quad + \underbrace{h_{1,1}b_{j+2,k+1} + h_{1,0}b_{j+2,k} + h_{1,1}b_{j+2,k-1}}_{\text{ITI signal from the } (j+1)\text{th track}}, \end{aligned} \quad (9)$$

respectively. It is clear that there is only one-side ITI effect that remains in the refined readback signals.

For the second turbo iteration onwards ($N_T \geq 2$), the switches in Fig. 2 are moved to the position **B**. To further lessen the ITI embedded in the 1st readback signal, we use the soft information λ_k^2 obtained from the LDPC decoder to reconstruct the estimated ITI signal, \tilde{c}_k^2 , which will be utilized to subtract from the 1st readback signal. Similarly, we also utilize the soft information λ_k^1 to generate the estimated ITI signal, \tilde{c}_k^1 , which will be employed to subtract from the 2nd readback signal to mitigate the ITI effect. Accordingly, the refined readback signals of the 1st and 2nd read heads can be obtained by

$$r_k^1 = y_k^1 - \tilde{c}_k^2, \quad (10)$$

$$r_k^2 = y_k^2 - \tilde{c}_k^1, \quad (11)$$

where \tilde{c}_k^m for $m \in \{1, 2\}$ is the soft ITI signal associated with the m th track and the k th data bit.

It has been shown in Appendix that for a symmetric target, the soft ITI signal \tilde{c}_k^m can be computed from

$$\tilde{c}_k^m = \left(\frac{W + X + Y + Z}{4 \cosh(\lambda_k^m/2) \cosh(\lambda_{k-1}^m/2) \cosh(\lambda_{k-2}^m/2)} \right), \quad (12)$$

where

$$W = x \sinh\left(\frac{\lambda_k^m + \lambda_{k-1}^m + \lambda_{k-2}^m}{2}\right), \quad (13)$$

$$X = y \sinh\left(\frac{\lambda_k^m + \lambda_{k-1}^m - \lambda_{k-2}^m}{2}\right), \quad (14)$$

$$Y = y \sinh\left(\frac{-\lambda_k^m + \lambda_{k-1}^m + \lambda_{k-2}^m}{2}\right), \quad (15)$$

$$Z = z \sinh\left(\frac{\lambda_k^m - \lambda_{k-1}^m + \lambda_{k-2}^m}{2}\right), \quad (16)$$

where λ_k^m is the LLR from the m th head of the k th bit at the LDPC decoder output.

B. TARGET AND EQUALIZER DESIGN

In a conventional system, because the readback signal generally contains the two-side ITI effect from the upper and lower tracks, the 3×3 target or full complexity trellis's structure (64 states with 8 incoming/outgoing branches) must be employed in a 2D SOVA detector. Nevertheless, with the proposed technique, the refined readback signals in (8) and (9) contain only the one-side ITI effect. Thus, we can utilize the 2×3 target so as to decrease the detector's complexity, which has only 16 states with 4 incoming/outgoing branches [20]. Consequently, this section briefly summarizes how to design the 2×3 target and its compatible 1D equalizer based on an MMSE approach [25].

Consider the BPMR channel model in Fig. 2. Let \mathbf{G}_1 and \mathbf{G}_2 be the 2×3 target, and \mathbf{f}_1 and \mathbf{f}_2 be the 1D equalizer associated with the 1st and 2nd read heads, respectively. To design for \mathbf{G}_1 and \mathbf{f}_1 , we write the target \mathbf{G}_1 in a matrix form as

$$\mathbf{G}_1 = \begin{bmatrix} \mathbf{g}_{-1} \\ \mathbf{g}_0 \end{bmatrix} = \begin{bmatrix} g_{-1,-1} & g_{-1,0} & g_{-1,1} \\ g_{0,-1} & g_{0,0} & g_{0,1} \end{bmatrix}. \quad (17)$$

Let $\mathbf{f} = [f_{-N} \dots f_0 \dots f_N]^T$ be a column vector of the equalizer \mathbf{f}_1 , $\mathbf{g} = [g_{-1,-1} \ g_{0,-1} \ g_{-1,0} \ g_{0,0} \ g_{-1,1} \ g_{0,1}]^T$ be a column vector of the target \mathbf{G}_1 , where $[\cdot]^T$ is the transpose operator, $g_{0,0}$ is set to be 1, $M = 2N + 1$ is the total number of equalizer taps, and the length of \mathbf{g} is $L = 6$. Therefore, \mathbf{f} and \mathbf{g} can be obtained by minimizing a mean-squared error (MSE) of the 1st read head, e_k^1 , between an equalizer output and a desired output according to

$$E \left[\{e_k^1\}^2 \right] = E \left[(\mathbf{f}^T \mathbf{r}_k - \mathbf{g}^T \mathbf{b}_k) (\mathbf{f}^T \mathbf{r}_k - \mathbf{g}^T \mathbf{b}_k)^T \right], \quad (18)$$

where $E[\cdot]$ is an expectation operator, $\mathbf{b}_k = [b_{0,k} \ b_{1,k} \ b_{0,k-1} \ b_{1,k-1} \ b_{0,k-2} \ b_{1,k-2}]^T$ is a column vector of a binary input sequence $\{b_{j,k}\}$, and $\mathbf{r}_k = [r_{k+N}^1 \ \dots \ r_k^1 \ \dots \ r_{k-N}^1]^T$ is a column vector of an equalizer input sequence $\{r_k^1\}$.

During the minimization process, a monic constraint must be imposed by setting $\mathbf{I}^T \mathbf{g} = 1$ to avoid the answer of $\mathbf{g} = \mathbf{f} = \mathbf{0}$. Thus, (18) can be rewritten as

$$E \left[\{e_k^1\}^2 \right] = \mathbf{f}^T \mathbf{R} \mathbf{f} + \mathbf{g}^T \mathbf{B} \mathbf{g} - 2 \mathbf{f}^T \mathbf{T} \mathbf{g} - 2\nu (\mathbf{I}^T \mathbf{g} - 1), \quad (19)$$

where $\mathbf{I} = [0 \ 0 \ 0 \ 1 \ 0 \ 0]^T$, ν is a Lagrange multiplier, $\mathbf{R} = E[\mathbf{r}_k \mathbf{r}_k^T]$ is an $M \times M$ auto-correlation matrix of $\{r_k^1\}$, $\mathbf{T} = E[\mathbf{r}_k \mathbf{b}_k^T]$ is an $M \times L$ cross-correlation matrix of $\{r_k^1\}$ and $\{b_{j,k}\}$, and $\mathbf{B} = E[\mathbf{b}_k \mathbf{b}_k^T]$ is an $L \times L$ auto-correlation matrix of $\{b_{j,k}\}$. By minimizing (19) with respect to ν , \mathbf{g} and \mathbf{f} , one obtains

$$\nu = \frac{1}{\mathbf{I}^T (\mathbf{B} - \mathbf{T}^T \mathbf{R}^{-1} \mathbf{T})^{-1} \mathbf{I}}, \quad (20)$$

$$\mathbf{g} = \nu (\mathbf{B} - \mathbf{T}^T \mathbf{R}^{-1} \mathbf{T})^{-1} \mathbf{I}, \quad (21)$$

$$\mathbf{f} = \mathbf{R}^{-1} \mathbf{T} \mathbf{g}. \quad (22)$$

For a symmetric channel without media noise and TMR, we can employ the equalizer $\mathbf{f}_2 = \mathbf{f}_1$ and the target \mathbf{G}_2 equal

to a flipped version of \mathbf{G}_1 according to

$$\mathbf{G}_2 = \begin{bmatrix} \mathbf{g}_0 \\ \mathbf{g}_{-1} \end{bmatrix} = \begin{bmatrix} g_{0,-1} & g_{0,0} & g_{0,1} \\ g_{-1,-1} & g_{-1,0} & g_{-1,1} \end{bmatrix}. \quad (23)$$

It should be pointed out that because the refined readback signals contain less ITI, the 1D equalizer and the 2×3 target should be redesigned for each turbo iteration ($N_T \geq 2$). However, we found that we can still use a new set of the target and its equalizer designed at $N_T = 2$ for $N_T > 2$ because no significant performance improvement can be acquired (will be demonstrated in Section IV).

IV. NUMERICAL RESULT

Consider the coded BPMR channel in Fig. 2. We evaluate the system performance at the ADs of 2, 2.5, and 3 Tb/in² corresponding to $T_x = T_z = 18$ nm, $T_x = T_z = 16$ nm, and $T_x = T_z = 14.5$ nm [9], respectively. Each island in Fig. 1 is a square island with 11 nm for each side. This article considers the fly height between a read head and a magnetic medium of 10 nm, a gap-to-gap width is 16 nm, the along-track PW_{50} (W_x) is 19.8 nm, and the cross-track PW_{50} (W_z) is 24.8 nm. Moreover, for the system without media noise and TMR, the weighting factor in (7) used in our system for the AD of 2, 2.5, and 3 Tb/in² is $\alpha = 0.2321$, $\alpha = 0.3154$, and $\alpha = 0.3876$, respectively.

Here, the signal-to-noise ratio (SNR) is defined as

$$\text{SNR} = 10 \log_{10} \left(\frac{1}{R\sigma^2} \right) \quad (24)$$

in decibel (dB), where $R = 8/9$ is a code rate of the LDPC code. We also employ the 7-tap ($M = 7$) equalizer designed based on the MMSE approach [25], where the target and its equalizer are designed at the SNR to achieve BER of about 10^{-4} for the uncoded system without media noise and TMR. In addition, a block of 3640 information bits is encoded by a regular (3, 27) LDPC code [23] to obtain a coded block of length 4095 bits, where the parity-check matrix has 3 ones in each column and 27 ones in each row. Finally, each BER point is computed based on a minimum number of 10000 coded blocks and 1000 error bits.

First, we investigate the proposed technique whether or not it is essential to redesign the equalizer and its compatible target for every turbo iteration. To do so, let S^j denotes a set of the equalizer and its compatible target designed at the j th iteration and by default used it only at the j th iteration (unless otherwise stated). For example, at AD = 2.5 Tb/in² and SNR = 10.63 dB, Fig. 3 demonstrates that redesigning S^j for every iteration can gradually improve the system performance, where "Use S^j for the j th iteration onwards" means that the system utilizes the same S^j for the i th iteration and $i = \{j, j+1, j+2, \dots\}$. Additionally, $N_T = 0.5$ is referred to as the system performance at the output of the 2D SOVA detector at the 1st iteration. It is apparent that the performance improvement is not considerable if S^2 is fixed and is employed for the i th iteration and $i = \{2, 3, 4, \dots\}$. Therefore, from this point on, we consider only the system

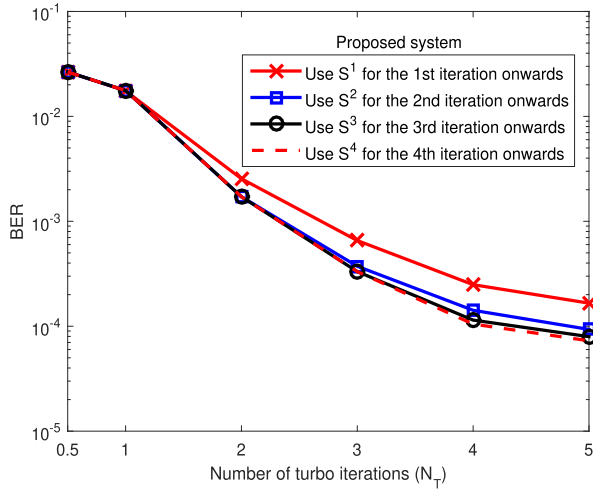


FIGURE 3. Performance of the proposed system with redesigning the equalizer and its compatible target for every turbo iteration.

that redesigns a new set of the equalizer and its target at the 2nd iteration (i.e., S^2) and uses it for the remaining turbo iterations so as to reduce the memory required to store the equalizers and targets of all iterations.

Then, we explore the performance of the proposed system as a function of the number of turbo iterations (N_T 's) at the AD of 2.5 and 3 Tb/in², as depicted in Fig. 4. Apparently, the BER performance gets better as N_T goes. Nevertheless, we found that the performance improvement is very small, when the number of turbo iterations is more than 5 iterations. As a result, from this point on, all systems will be evaluated at the 5th turbo iteration ($N_T = 5$).

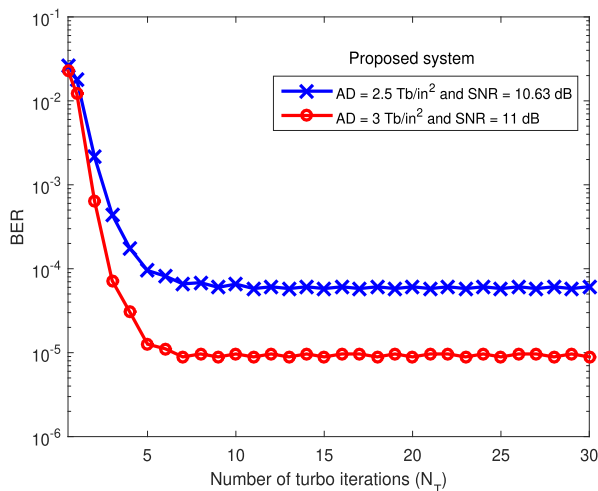


FIGURE 4. Performance of the proposed system as a function of N_T 's.

Next, we compare the BER performance of different systems at the AD of 2, 2.5, and 3 Tb/in² in Fig. 5, where the performance of the proposed system is denoted as “Proposed (DTDH with soft decision)” and that of the system in [20] using a hard ITI mitigation technique is referred to as “DTDH with hard decision.” For the conventional system that employs a single read head and decode one single track,

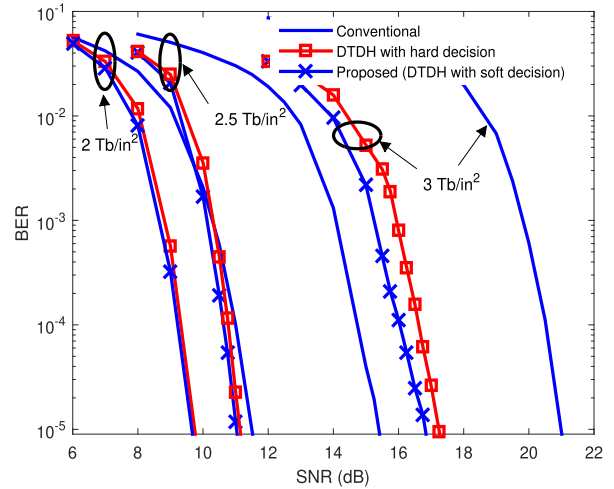


FIGURE 5. Performance comparison at different ADs.

we denote it as “Conventional.” Note that in the SOVA detector, the conventional system employs the 3×3 target whose trellis has 64 states with 8 incoming/outgoing branches at each state, whereas the DTDH system can utilize the 2×3 target. As depicted in Fig. 5, the proposed system performs the best for all ADs, especially at high ADs. For instance, at AD = 3 Tb/in² and BER = 10^{-5} , it is clear that “Proposed (DTDH with soft decision)” can provide a performance gain of about 0.4 and 5.2 dBs over “DTDH with hard decision” and “Conventional,” respectively. This is because the proposed technique can estimate the ITI signal better than the hard ITI suppression technique.

To confirm that the proposed system can estimate the ITI signal well, we measure the MSE between the actual ITI signal, c_k^m , and the estimated one, \tilde{c}_k^m , according to

$$MSE = 10 \log_{10} \left(\frac{1}{B} \sum_{k=1}^B (c_k^m - \tilde{c}_k^m)^2 \right), \quad (25)$$

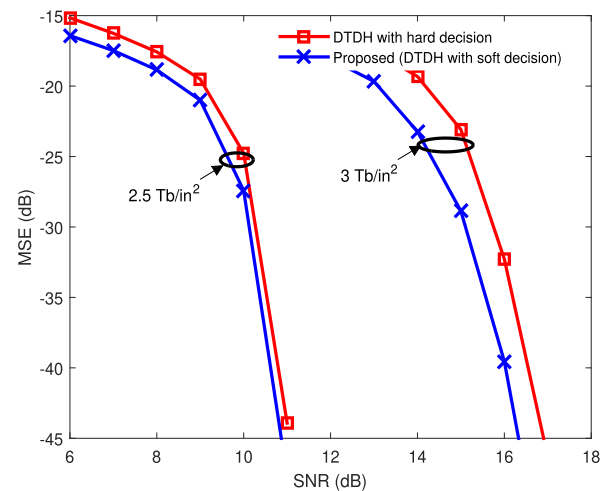


FIGURE 6. MSE performance as a function of SNRs.

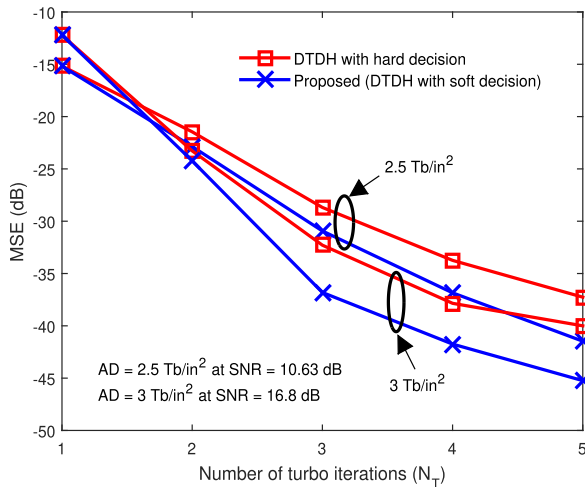


FIGURE 7. MSE performance as a function of N_T 's.

in dB, where $B = 4095$ is the length of a coded data sector. Fig. 6 compares the MSE between the system using soft ITI suppression technique (i.e., the proposed system) and that using hard ITI suppression technique (denoted as “DTDH with hard decision”) as a function of SNRs. Apparently, the proposed system yields lower MSE than “DTDH with hard decision,” especially at high ADs. Furthermore, we also compare the MSE of both systems as a function of a number of turbo iterations (N_T) in Fig. 7, where we use SNR = 10.63 and 16.8 dB for AD = 2.5 and 3 Tb/in^2 , corresponding to the proposed system having BER of 10^{-4} and 10^{-5} , respectively. Again, the proposed system provides lower MSE than “DTDH with hard decision” as N_T goes. For example, at AD = 3 Tb/in^2 and $N_T = 5$, the proposed system offers 5 dB lower than “DTDH with hard decision.” These results confirm why the proposed system is superior to “DTDH with hard decision.”

Moreover, we also investigate the system performance in the presence of media noise and TMR, which practically

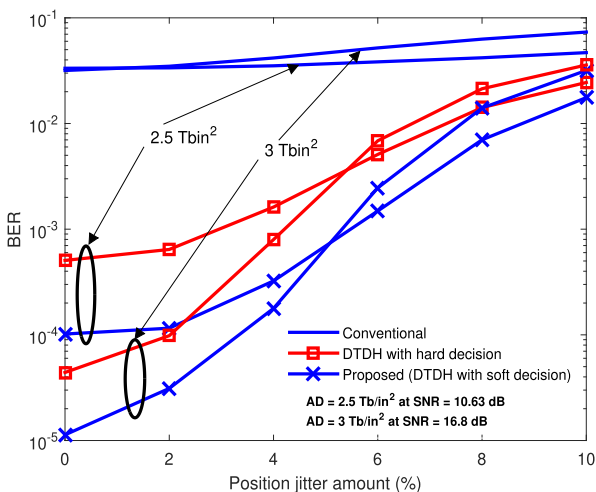


FIGURE 8. Performance comparison as a function of position jitter amounts.

occurs in real applications. Fig. 8 illustrates the performance comparison of several systems in the presence of position jitter noise. It reveals that the proposed system outperforms the other systems for all position jitter amounts (σ_j/T_x 's). For instance, at AD = 3 Tb/in^2 and $\sigma_j/T_x = 4\%$, the proposed system can provide the BER of 0.9 decade lower than “DTDH with hard decision” and is much superior to “Conventional.” Finally, the BER performance of different systems as a function of TMR amounts is compared in Fig. 9, where +TMR and -TMR denote the upward and downward directions, respectively. Clearly, the proposed system is more robust to TMR than “DTDH with hard decision,” and both DTDH systems outperform “Conventional.”

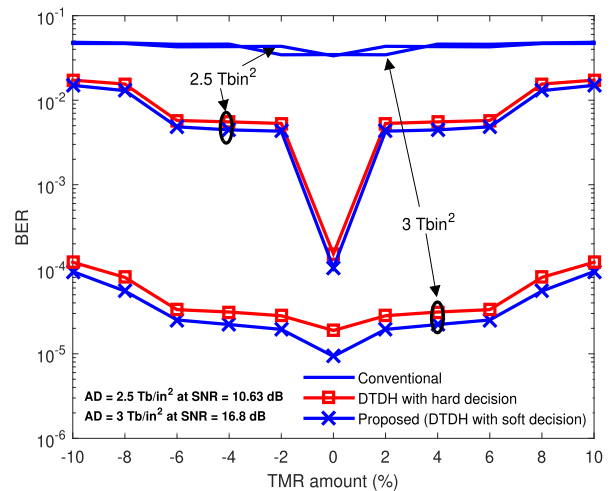


FIGURE 9. Performance comparison as a function of TMR amounts.

V. CONCLUSION

The ITI effect is a major problem in an ultra-high density BPMR system because it can deteriorate the overall system performance. To alleviate the ITI, we propose a novel ITI suppression technique for a coded DTDH BPMR system by utilizing the soft information of the adjacent track obtained from the LDPC decoder to estimate the ITI signal and subtracting it from the associated readback signal at each turbo iteration. As illustrated in the simulation results, the proposed system using the soft information from the LDPC decoder to estimate the ITI signal yields better performance than the DTDH system using the hard decision from the LDPC decoder to approximate the ITI signal. Nonetheless, the DTDH system using either a soft or a hard ITI suppression technique is superior to the conventional system that uses only one read head to decode one data track, particularly when AD is large. Furthermore, we found that the proposed system is also robust to TMR and media noise, if compared to both the DTDH system using a hard ITI suppression technique and the conventional system. Eventually, it should be pointed out that the proposed technique can also be applied for the m -track m -head ($m \geq 3$) detection in BPMR systems, as presented in [26].

TABLE 1. A relationship between the channel input and the channel output for a given channel.

Input $\{b_{m,k}, b_{m,k-1}, b_{m,k-2}\}$	Possible values		d_i
	Generalized target	Symmetric target	
$\{-1, -1, -1\}$	$-h_{-1,-1} - h_{-1,0} - h_{-1,1}$	$-2h - h_{-1,0}$	$-x$
$\{-1, -1, 1\}$	$-h_{-1,-1} - h_{-1,0} + h_{-1,1}$	$-h_{-1,0}$	$-y$
$\{-1, 1, -1\}$	$-h_{-1,-1} + h_{-1,0} - h_{-1,1}$	$-2h + h_{-1,0}$	$-z$
$\{-1, 1, 1\}$	$-h_{-1,-1} + h_{-1,0} + h_{-1,1}$	$h_{-1,0}$	y
$\{1, -1, -1\}$	$h_{-1,-1} - h_{-1,0} - h_{-1,1}$	$-h_{-1,0}$	$-y$
$\{1, -1, 1\}$	$h_{-1,-1} - h_{-1,0} + h_{-1,1}$	$2h - h_{-1,0}$	z
$\{1, 1, -1\}$	$h_{-1,-1} + h_{-1,0} - h_{-1,1}$	$h_{-1,0}$	y
$\{1, 1, 1\}$	$h_{-1,-1} + h_{-1,0} + h_{-1,1}$	$2h + h_{-1,0}$	x

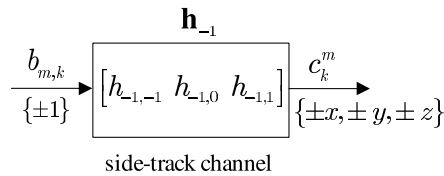


FIGURE 10. A side-track channel.

APPENDIX
GENERATING THE SOFT ITI SIGNAL

Consider a side-track channel in Fig. 10, where the binary input bits $b_{m,k} \in \{-1, 1\}$ are independent and identically distributed random variables. Then, a sequence $\{b_{m,k}\}$ is filtered by the side-track channel, \mathbf{h}_{-1} , given by

$$\mathbf{h}_{-1}(D) = \sum_{k=-1}^1 h_{-1,k} D^k = h_{-1,-1} D^{-1} + h_{-1,0} + h_{-1,1} D, \quad (A.1)$$

where D is a delay operator, to obtain a channel output sequence $\{c_k^m\}$ according to

$$c_k^m = b_{m,k} * \mathbf{h}_{-1}, \quad (A.2)$$

and $*$ is an 1D convolution operator. For a symmetric channel without TMR and media noise, it can be shown that $c_k^m \in \{\pm x, \pm y, \pm z\}$, where $x = 2h + h_{-1,0}$, $y = h_{-1,0}$, $z = 2h - h_{-1,0}$, and $h = h_{-1,-1} = h_{-1,1}$, as given in Table 1.

At a receiver side, a conventional turbo decoder for the side-track channel provides the LLRs, $\{\lambda_k^m\}$, for the channel input sequence $\{b_{m,k}\}$. Consider a memoryless soft slicer that utilizes the LLRs $\{\lambda_k^m\}$ to output a soft decision $\tilde{c}_k^m = E[c_k^m | \{\lambda_k^m\}]$, which can be calculated from

$$\begin{aligned} \tilde{c}_k^m &= \sum_i d_i \Pr[c_k^m = d_i | \{\lambda_k^m\}] \\ &= x \Pr[c_k^m = x | \{\lambda_k^m\}] + y \Pr[c_k^m = y | \{\lambda_k^m\}] \\ &\quad + z \Pr[c_k^m = z | \{\lambda_k^m\}] - x \Pr[c_k^m = -x | \{\lambda_k^m\}] \\ &\quad - y \Pr[c_k^m = -y | \{\lambda_k^m\}] \\ &\quad - z \Pr[c_k^m = -z | \{\lambda_k^m\}], \end{aligned} \quad (A.3)$$

where $d_i \in \{\pm x, \pm y, \pm z\}$ is illustrated in Table 1. Let the LLR, λ_k^m , of the input bit, $b_{m,k}$, be given by

$$\lambda_k^m = \log \left(\frac{\Pr[b_{m,k} = 1 | \{\lambda_k^m\}]}{\Pr[b_{m,k} = -1 | \{\lambda_k^m\}]} \right). \quad (A.4)$$

Therefore, it is obvious to demonstrate that

$$\Pr[b_{m,k} = 1 | \{\lambda_k^m\}] = \frac{e^{\lambda_k^m/2}}{e^{\lambda_k^m/2} + e^{-\lambda_k^m/2}}, \quad (A.5)$$

$$\Pr[b_{m,k} = -1 | \{\lambda_k^m\}] = \frac{e^{-\lambda_k^m/2}}{e^{\lambda_k^m/2} + e^{-\lambda_k^m/2}}. \quad (A.6)$$

To obtain the channel output $c_k^m = -x$, the channel input must be $\{b_{m,k}, b_{m,k-1}, b_{m,k-2}\} = \{-1, -1, -1\}$. Thus, we obtain

$$\begin{aligned} \Pr[c_k^m = -x | \lambda_k^m] &= \Pr[b_{m,k} = -1 | \lambda_k^m] \\ &\quad \times \Pr[b_{m,k-1} = -1 | \lambda_k^m] \\ &\quad \times \Pr[b_{m,k-2} = -1 | \lambda_k^m] \\ &= \left(\frac{e^{-\lambda_k^m/2}}{e^{\lambda_k^m/2} + e^{-\lambda_k^m/2}} \right) \\ &\quad \times \left(\frac{e^{-\lambda_{k-1}^m/2}}{e^{\lambda_{k-1}^m/2} + e^{-\lambda_{k-1}^m/2}} \right) \\ &\quad \times \left(\frac{e^{-\lambda_{k-2}^m/2}}{e^{\lambda_{k-2}^m/2} + e^{-\lambda_{k-2}^m/2}} \right). \end{aligned} \quad (A.7)$$

Next, the channel input must be $\{b_{m,k}, b_{m,k-1}, b_{m,k-2}\} = \{1, 1, 1\}$ to produce the channel output $c_k^m = x$. Then, we get

$$\begin{aligned} \Pr[c_k^m = x | \lambda_k^m] &= \Pr[b_{m,k} = 1 | \lambda_k^m] \\ &\quad \times \Pr[b_{m,k-1} = 1 | \lambda_k^m] \\ &\quad \times \Pr[b_{m,k-2} = 1 | \lambda_k^m] \\ &= \left(\frac{e^{\lambda_k^m/2}}{e^{\lambda_k^m/2} + e^{-\lambda_k^m/2}} \right) \\ &\quad \times \left(\frac{e^{\lambda_{k-1}^m/2}}{e^{\lambda_{k-1}^m/2} + e^{-\lambda_{k-1}^m/2}} \right) \\ &\quad \times \left(\frac{e^{\lambda_{k-2}^m/2}}{e^{\lambda_{k-2}^m/2} + e^{-\lambda_{k-2}^m/2}} \right). \end{aligned} \quad (A.8)$$

Similarly, to obtain the channel output $c_k^m = -y$, the channel input must be $\{b_{m,k}, b_{m,k-1}, b_{m,k-2}\} = \{-1, -1, 1\}$ or $\{1, -1, -1\}$. Hence, we acquire

$$\begin{aligned} \Pr[c_k^m = -y | \lambda_k^m] &= \{\Pr[b_{m,k} = -1 | \lambda_k^m] \\ &\quad \times \Pr[b_{m,k-1} = -1 | \lambda_k^m] \\ &\quad \times \Pr[b_{m,k-2} = 1 | \lambda_k^m]\} \end{aligned}$$

$$\begin{aligned}
 & + \{ \Pr [b_{m,k} = 1 | \lambda_k^m] \\
 & \times \Pr [b_{m,k-1} = -1 | \lambda_k^m] \\
 & \times \Pr [b_{m,k-2} = -1 | \lambda_k^m] \} \\
 = & \left\{ \left(\frac{e^{-\lambda_k^m/2}}{e^{\lambda_k^m/2} + e^{-\lambda_k^m/2}} \right) \right. \\
 & \times \left(\frac{e^{-\lambda_{k-1}^m/2}}{e^{\lambda_{k-1}^m/2} + e^{-\lambda_{k-1}^m/2}} \right) \\
 & \times \left(\frac{e^{\lambda_{k-2}^m/2}}{e^{\lambda_{k-2}^m/2} + e^{-\lambda_{k-2}^m/2}} \right) \left. \right\} \\
 & + \left\{ \left(\frac{e^{\lambda_k^m/2}}{e^{\lambda_k^m/2} + e^{-\lambda_k^m/2}} \right) \right. \\
 & \times \left(\frac{e^{-\lambda_{k-1}^m/2}}{e^{\lambda_{k-1}^m/2} + e^{-\lambda_{k-1}^m/2}} \right) \\
 & \times \left. \left(\frac{e^{-\lambda_{k-2}^m/2}}{e^{\lambda_{k-2}^m/2} + e^{-\lambda_{k-2}^m/2}} \right) \right\}. \quad (A.9)
 \end{aligned}$$

Sequentially, the channel input must be $\{b_{m,k}, b_{m,k-1}, b_{m,k-2}\} = \{1, 1, -1\}$ or $\{-1, 1, 1\}$ to generate the channel output $c_k^m = y$. Thus, we obtain

$$\begin{aligned}
 \Pr [c_k^m = x | \lambda_k^m] = & \{ \Pr [b_{m,k} = -1 | \lambda_k^m] \\
 & \times \Pr [b_{m,k-1} = 1 | \lambda_k^m] \\
 & \times \Pr [b_{m,k-2} = 1 | \lambda_k^m] \} \\
 & + \{ \Pr [b_{m,k} = 1 | \lambda_k^m] \\
 & \times \Pr [b_{m,k-1} = 1 | \lambda_k^m] \\
 & \times \Pr [b_{m,k-2} = -1 | \lambda_k^m] \} \\
 = & \left\{ \left(\frac{e^{-\lambda_k^m/2}}{e^{\lambda_k^m/2} + e^{-\lambda_k^m/2}} \right) \right. \\
 & \times \left(\frac{e^{\lambda_{k-1}^m/2}}{e^{\lambda_{k-1}^m/2} + e^{-\lambda_{k-1}^m/2}} \right) \\
 & \times \left(\frac{e^{\lambda_{k-2}^m/2}}{e^{\lambda_{k-2}^m/2} + e^{-\lambda_{k-2}^m/2}} \right) \left. \right\} \\
 & + \left\{ \left(\frac{e^{\lambda_k^m/2}}{e^{\lambda_k^m/2} + e^{-\lambda_k^m/2}} \right) \right. \\
 & \times \left(\frac{e^{\lambda_{k-1}^m/2}}{e^{\lambda_{k-1}^m/2} + e^{-\lambda_{k-1}^m/2}} \right) \\
 & \times \left. \left(\frac{e^{-\lambda_{k-2}^m/2}}{e^{\lambda_{k-2}^m/2} + e^{-\lambda_{k-2}^m/2}} \right) \right\}. \quad (A.10)
 \end{aligned}$$

Next, to obtain the channel output $c_k^m = -z$, the channel input must be $\{b_{m,k}, b_{m,k-1}, b_{m,k-2}\} = \{-1, 1, -1\}$. Then, we get

$$\begin{aligned}
 \Pr [c_k^m = x | \lambda_k^m] = & \Pr [b_{m,k} = -1 | \lambda_k^m] \\
 & \times \Pr [b_{m,k-1} = 1 | \lambda_k^m] \\
 & \times \Pr [b_{m,k-2} = -1 | \lambda_k^m]
 \end{aligned}$$

$$\begin{aligned}
 = & \left(\frac{e^{-\lambda_k^m/2}}{e^{\lambda_k^m/2} + e^{-\lambda_k^m/2}} \right) \\
 & \times \left(\frac{e^{\lambda_{k-1}^m/2}}{e^{\lambda_{k-1}^m/2} + e^{-\lambda_{k-1}^m/2}} \right) \\
 & \times \left(\frac{e^{-\lambda_{k-2}^m/2}}{e^{\lambda_{k-2}^m/2} + e^{-\lambda_{k-2}^m/2}} \right). \quad (A.11)
 \end{aligned}$$

Finally, to obtain the channel output $c_k^m = z$, the channel input must be $\{b_{m,k}, b_{m,k-1}, b_{m,k-2}\} = \{1, -1, 1\}$. Hence, we acquire

$$\begin{aligned}
 \Pr [c_k^m = x | \lambda_k^m] = & \Pr [b_{m,k} = 1 | \lambda_k^m] \\
 & \times \Pr [b_{m,k-1} = -1 | \lambda_k^m] \\
 & \times \Pr [b_{m,k-2} = 1 | \lambda_k^m] \\
 = & \left(\frac{e^{\lambda_k^m/2}}{e^{\lambda_k^m/2} + e^{-\lambda_k^m/2}} \right) \\
 & \times \left(\frac{e^{-\lambda_{k-1}^m/2}}{e^{\lambda_{k-1}^m/2} + e^{-\lambda_{k-1}^m/2}} \right) \\
 & \times \left(\frac{e^{\lambda_{k-2}^m/2}}{e^{\lambda_{k-2}^m/2} + e^{-\lambda_{k-2}^m/2}} \right). \quad (A.12)
 \end{aligned}$$

Let $a = \lambda_k^m/2$, $b = \lambda_{k-1}^m/2$, and $c = \lambda_{k-2}^m/2$. By substituting (A.7) – (A.12) into (A.3), one obtains

$$c_k^m = \frac{\begin{pmatrix} -xe^{-a}e^{-b}e^{-c} + xe^ae^be^c - ye^{-a}e^{-b}e^c \\ -ye^ae^{-b}e^{-c} + ye^{-a}e^be^c + ye^ae^be^{-c} \\ -ze^{-a}e^be^{-c} + ze^ae^{-b}e^c \end{pmatrix}}{(e^a + e^{-a})(e^b + e^{-b})(e^c + e^{-c})}. \quad (A.13)$$

Because $\cosh(\theta) = \frac{e^\theta + e^{-\theta}}{2}$ and $\sinh(\theta) = \frac{e^\theta - e^{-\theta}}{2}$, (A.13) reduces to

$$\begin{aligned}
 c_k^m = & \frac{\begin{pmatrix} -xe^{-a}e^{-b}e^{-c} + xe^ae^be^c - ye^{-a}e^{-b}e^c \\ -ye^ae^{-b}e^{-c} + ye^{-a}e^be^c + ye^ae^be^{-c} \\ -ze^{-a}e^be^{-c} + ze^ae^{-b}e^c \end{pmatrix}}{8 \cosh(a) \cosh(b) \cosh(c)} \\
 = & \frac{\begin{pmatrix} -xe^{-(a+b+c)} + xe^{(a+b+c)} - ye^{-(a+b-c)} \\ + ye^{(a+b-c)} - ye^{-(a+b+c)} + ye^{-(a+b+c)} \\ -ze^{-(a-b+c)} + ze^{(a-b+c)} \end{pmatrix}}{8 \cosh(a) \cosh(b) \cosh(c)} \\
 = & \frac{\begin{pmatrix} -x \sinh(a+b+c) + y \sinh(a+b-c) \\ + y \sinh(-a+b+c) + z \sinh(a-b+c) \end{pmatrix}}{4 \cosh(a) \cosh(b) \cosh(c)}. \quad (A.14)
 \end{aligned}$$

Again, by substituting $a = \lambda_k^m/2$, $b = \lambda_{k-1}^m/2$, and $c = \lambda_{k-2}^m/2$ in (A.14), we obtain

$$\begin{aligned}
 \tilde{c}_k^m = & \frac{\begin{pmatrix} x \sinh \left(\frac{\lambda_k^m + \lambda_{k-1}^m + \lambda_{k-2}^m}{2} \right) \\ + y \sinh \left(\frac{\lambda_k^m + \lambda_{k-1}^m - \lambda_{k-2}^m}{2} \right) \\ + y \sinh \left(\frac{-\lambda_k^m + \lambda_{k-1}^m + \lambda_{k-2}^m}{2} \right) \\ + z \sinh \left(\frac{\lambda_k^m - \lambda_{k-1}^m + \lambda_{k-2}^m}{2} \right) \end{pmatrix}}{4 \cosh(\lambda_k^m/2) \cosh(\lambda_{k-1}^m/2) \cosh(\lambda_{k-2}^m/2)}, \quad (A.15)
 \end{aligned}$$

which is same as (12).

ACKNOWLEDGMENT

The authors would like to thank the anonymous reviewers for their valuable comments.

REFERENCES

- [1] H. J. Richter, A. Y. Dobin, O. Heinonen, K. Z. Gao, R. J. M. Van de Veerdonk, R. T. Lynch, J. Xue, D. Weller, P. Asselin, M. F. Erden, and R. M. Brockie, "Recording on bit-patterned media at densities of 1 Tb/in² and beyond," *IEEE Trans. Magn.*, vol. 42, no. 10, pp. 2255–2260, Oct. 2006.
- [2] Y. Shiroishi, K. Fukuda, I. Tagawa, H. Iwasaki, S. Takenoiri, H. Tanaka, H. Mutoh, and N. Yoshikawa, "Future options for HDD storage," *IEEE Trans. Magn.*, vol. 45, no. 10, pp. 3816–3822, Oct. 2009.
- [3] S. Nabavi and B. V. K. V. Kumar, "Two-dimensional generalized partial response equalizer for bit-patterned media," in *Proc. IEEE Int. Conf. Commun. (ICC)*, Jun. 2007, pp. 6249–6254.
- [4] Y. Ng, B. V. K. Vijaya Kumar, K. Cai, S. Nabavi, and T. C. Chong, "Picket-shift codes for bit-patterned media recording with Insertion/Deletion errors," *IEEE Trans. Magn.*, vol. 46, no. 6, pp. 2268–2271, Jun. 2010.
- [5] K. Weisen, R. M. Lansky, and C. Sobey, "Recording asymmetries at large skew angles," *IEEE Trans. Magn.*, vol. 29, no. 6, pp. 4002–4004, Nov. 1993.
- [6] A. R. Iyengar, P. H. Siegel, and J. K. Wolf, "Write channel model for bit-patterned media recording," *IEEE Trans. Magn.*, vol. 47, no. 1, pp. 35–45, Jan. 2011.
- [7] D. K. Min, H. S. Oh, and I. K. Yoo, "New data detection method for a HDD with patterned media," in *Proc. 7th IEEE Conf. Sensors*, Oct. 2008, pp. 1064–1067.
- [8] S. Nabavi, B. V. K. V. Kumar, and J.-G. Zhu, "Modifying Viterbi algorithm to mitigate intertrack interference in bit-patterned media," *IEEE Trans. Magn.*, vol. 43, no. 6, pp. 2274–2276, Jun. 2007.
- [9] M. Keskinöz, "Two-dimensional equalization/detection for patterned media storage," *IEEE Trans. Magn.*, vol. 44, no. 4, pp. 533–539, Apr. 2008.
- [10] S. Karakulak, "From channel modeling to signal processing for bit-patterned media recording," Ph.D. dissertation, Dept. Elect. Eng., Univ. California, San Diego, San Diego, CA, USA, 2010.
- [11] C. Warisarn, A. Arrayangkool, and P. Kovintavewat, "An ITI-mitigating 5/6 modulation code for bit-patterned media recording," *IEICE Trans. Electron.*, vol. E98.C, no. 6, pp. 528–533, Jun. 2015.
- [12] P. Kovintavewat, A. Arrayangkool, and C. Warisarn, "A rate-8/9 2-D modulation code for bit-patterned media recording," *IEEE Trans. Magn.*, vol. 50, no. 11, Nov. 2014, Art. no. 3101204.
- [13] W. Chang and J. R. Cruz, "Intertrack interference mitigation on staggered bit-patterned media," *IEEE Trans. Magn.*, vol. 47, no. 10, pp. 2551–2554, Oct. 2011.
- [14] M. Fujii and N. Shinohara, "Multi-track iterative ITI canceller for shingled write recording," in *Proc. 10th Int. Symp. Commun. Inf. Technol. (ISCIT)*, Oct. 2010, pp. 1062–1067.
- [15] J. Yao, K. C. Teh, and K. H. Li, "Performance evaluation of maximum-likelihood page detection for 2-D interference channel," *IEEE Trans. Magn.*, vol. 48, no. 7, pp. 2239–2242, Jul. 2012.
- [16] G. Mathew, E. Hwang, J. Park, G. Garfunkel, and D. Hu, "Capacity advantage of array-reader-based magnetic recording (ARMR) for next generation hard disk drives," *IEEE Trans. Magn.*, vol. 50, no. 3, pp. 155–161, Mar. 2014.
- [17] J. Yao, E. Hwang, B. V. K. V. Kumar, and G. Mathew, "Two-track joint detection for two-dimensional magnetic recording (TDMR)," in *Proc. IEEE Int. Conf. Commun. (ICC)*, Jun. 2015, pp. 418–424.
- [18] S. Koonkarnkhai and P. Kovintavewat, "A simple 2-head 2-track detection method for bit-patterned magnetic recording systems," in *Proc. 18th Int. Symp. Commun. Inf. Technol. (ISCIT)*, Sep. 2018, pp. 490–494.
- [19] M. Tuchler, R. Koetter, and A. C. Singer, "Turbo equalization: Principles and new results," *IEEE Trans. Commun.*, vol. 50, no. 5, pp. 754–767, May 2002.
- [20] S. Koonkarnkhai, C. Warisarn, and P. Kovintavewat, "An iterative two-head two-track detection method for staggered bit-patterned magnetic recording systems," *IEEE Trans. Magn.*, vol. 55, no. 7, Jul. 2019, Art. no. 3001707.
- [21] P. Kovintavewat and S. Koonkarnkhai, "Joint TA suppression and turbo equalization for coded partial response channels," *IEEE Trans. Magn.*, vol. 46, no. 6, pp. 1393–1396, Jun. 2010.
- [22] S. Koonkarnkhai, C. Warisarn, N. Chirdchoo, and P. Kovintavewat, "A soft ITI mitigation method for coded 2H2T BPMR systems," in *Proc. 34th Int. Tech. Conf. Circuits/Syst., Comput. Commun. (ITC-CSCC)*, Jun. 2019, pp. 1–3.
- [23] R. G. Gallager, "Low-density parity-check codes," *IRE Trans. Inf. Theory*, vol. IT-8, no. 1, pp. 21–28, Jan. 1962.
- [24] J. Hagenauer and P. Hoeher, "A Viterbi algorithm with soft-decision outputs and its applications," in *Proc. IEEE Global Telecommun. Conf. (GLOBECOM)*, Nov. 1989, pp. 1680–1686.
- [25] J. Moon and W. Zeng, "Equalization for maximum likelihood detectors," *IEEE Trans. Magn.*, vol. 31, no. 2, pp. 1083–1088, Mar. 1995.
- [26] S. Koonkarnkhai and P. Kovintavewat, "An iterative ITI cancellation method for multi-head multi-track bit-patterned magnetic recording systems," *Digit. Commun. Netw.*, Feb. 2020, doi: 10.1016/j.dcan.2020.02.003.



SANTI KOONKARNKHA received the B.Eng. degree in electronics engineering technology, and the M.Eng. and Ph.D. degrees in electrical engineering from the King Mongkut's University of Technology North Bangkok (KMUTNB), Thailand, in 2006, 2009, and 2014, respectively. Since 2011, he has continued his career with the Department of Electrical Engineering, Faculty of Science and Technology, Nakhon Pathom Rajabhat University (NPRU). His research interests include communication systems, detector, error-correction code (ECC), and signal processing for data storage systems.



CHANON WARISARN (Member, IEEE) received the B.Eng. degree (Hons.) in electronics engineering technology from the King Mongkut's Institute of Technology North Bangkok (KMUTNB), Thailand, in 2006, and the Ph.D. degree in electrical engineering from the King Mongkut's Institute of Technology Ladkrabang (KITL), Bangkok, Thailand, in 2011. He currently works with the College of Advanced Manufacturing Innovation (AMI), KITL. His current research interests include communications and signal processing for data storage systems.



PIYA KOVINTAVEWAT (Member, IEEE) received the B.Eng. degree (*summa cum laude*) from Thammasat University, Thailand, in 1994, the M.Sc. degree from the Chalmers University of Technology, Sweden, in 1998, and the Ph.D. degree from the Georgia Institute of Technology, USA, in 2004, all in electrical engineering. He is currently working with Nakhon Pathom Rajabhat University (NPRU). Prior to working at NPRU, he has worked as an Engineer with Thai Telephone and Telecommunication Company, Thailand, from 1994 to 1997, and a Research Assistant with the National Electronics and Computer Technology Center, Thailand, in 1999. He also had work experiences with Seagate Technology, Pennsylvania, USA, in summer of 2001, 2002, and 2004. His research interests include coding and signal processing as applied to digital data storage systems.